Chaos, Solitons and Fractals 171 (2023) 113459

Contents lists available at ScienceDirect

Chaos, Solitons and Fractals

journal homepage: www.elsevier.com/locate/chaos

Evolving cycles and self-organised criticality in social dynamics

Bosiljka Tadić [a,b], Marija Mitrović Dankulov [c,*], Roderick Melnik [d]

[a] Department for Theoretical Physics, Jožef Stefan Institute, Sl-1001, Ljubljana, Slovenia
[b] Complexity Science Hub, Vienna, Austria
[c] Institute of Physics Belgrade, University of Belgrade, Pregrevica 118, 11080 Belgrade, Serbia
[d] MS2Discovery Interdisciplinary Research Institute, Wilfrid Laurier University, Waterloo, ON, Canada

ARTICLE INFO

Keywords:
Social dynamics
Online social networks
Self-organised criticality
Social-activity avalanches
Cyclic trends
Multifractal fluctuations
Non-equilibrium dynamics

ABSTRACT

In many complex systems, self-organised criticality (SOC) provides a mechanism for the diversity of spatiotemporal scales that optimises the system's response to omnipresent driving forces. Signatures of SOC are increasingly more evidenced in collective social behaviours. However, the spontaneous occurrence of critical states and their role in maintaining the system's functional properties still need to be better understood; the reason can be related to the complexity of human interactions and the ubiquitous presence of cycles in social dynamics. In this work, we shed new light on these issues based on a critical survey and the extensive data analysis of online social dynamics. Firstly, we highlight prominent features of human activity patterns, conditioned by circadian cycles and content-related interactions, that can affect the course of the dynamics from the elemental to the global scale. We then analyse the prototypal time series of emotion-driven communications in the online social network `MySpace` to demonstrate the coexistence of SOC states with the modulated cyclical trends. Precisely, we determine avalanches of emotional comments exhibiting multifractal scaling, scale-invariant inter-avalanching behaviours and temporal correlations coexist with the cyclical trends of broad singularity spectra. We demonstrate that similar multi-harmonic cycles occur in entirely different datasets, particularly the negative emotion-driven `Diggs` and the infection-rate data from recent epidemics. Our results reveal the dynamical regime where the modulated cycles coexist with self-organised critical states; in contrast, in the cycles-dominated regime, exemplified by the infection time series, the nature of collective dynamics remains hidden behind the cycle modulation.

1. Introduction

In the nonlinear out-of-equilibrium dynamical systems, the term self-organised criticality (SOC) refers to the system's ability to reach a stationary state with long-range spatiotemporal correlations under repeated driving. Thus, SOC states appear as attractors of the underlying nonlinear dynamics in large systems consisting of many interacting elements exposed to various constraints and driving forces. They were first introduced and described in the prototypal sandpile automata models [1,2]. These critical states resemble ones near the second-order phase transitions and are reported in many physical, biological and social systems [3–6]. It was understood that, in naturally evolving systems, e.g. brain [7,8], geophysical [9] and astrophysical activity [4], these critical states provide the system's multi-scale response to the driving forces, thus maintaining its robustness and functional stability. In the research of biological systems, SOC is recently used to explain the mechanisms at work in engineering of living cells [10], cancerogenesis [11], and gene expressions leading to cancer-cell lines [12]. Furthermore, the formal properties of SOC states, e.g., in the dynamics of structured networks, appear as a key towards understanding spatiotemporal and information complexity; see a recent summary in [13] and references there. As discussed below, the SOC states are characterised by avalanches with scale-invariant distributions, temporal correlations and fractal features of time series; see a review in [14] and references there. Moreover, the expansion (or contraction) of the phase space [15,16] during the system's evolution leads to scaling of the ranking-order distributions, better known as Zipf's and Heap's laws [17], of different quantities.

In the context of the emergence of collective dynamics from individual actions and interactions, studies of human dynamics in real life and virtual space are particularly challenging. Motivations to understand collective human behaviours have practical challenges, e.g., to improve management in crises. Theoretically, wide variations of human features and diversity of interactions as well as the ability of self-organisation and collective learning of an involved community during the process

* Corresponding author.
E-mail address: mitrovic@ipb.ac.rs (M. Mitrović Dankulov).

https://doi.org/10.1016/j.chaos.2023.113459
Received 15 March 2023; Accepted 12 April 2023
Available online 3 May 2023

makes direct applications of physics theories of nonlinear driven systems to the studies of social dynamics inappropriate. See the Ref. [18] for a recent overview of modified theoretical concepts for studying human crowds in real space. On the other hand, the massive amount of data from online social sites provides a unique opportunity to analyse human dynamics via advanced data analysis and agent-based modelling [19]. The absence of physical space and the ease of communications in the online world imply some fundamental differences compared to real-world social phenomena [19,20]. Nevertheless, it is tempting to believe that studies of online social dynamics can provide a deeper understanding of human collective behaviours.

Many signatures of SOC states are increasingly discovered in collective dynamics extracted from the online social interactions data at different sites, and confirmed by data-related agent-based simulations, in particular in MySpace [21–23], Blogs [24–26], Diggs [27,28], IR chats Ubuntu [29], Mathematics Questions-and-Answers [16,30], Twitter [31,32], and others. Recently, the concepts of SOC have been intensively used to analyse the data relating to real-world social systems from the organisation and developments of cities [33,34] to the interpretation of social equilibrium [35], economy [36] and epidemiology [37] crisis. Other studies used the concept of SOC to describe data related to psychological disorders [38], political behaviours and rebellions [39,40], and wars [41] as well as the evolution of different societies, languages, economic inequalities and the entire history [42–45]. A theoretical concept of SOC approaching big data is beneficial in this context. Firstly, the amount of data necessary to find a reliable pattern can be considerably reduced by detecting the underlying scale invariance due to SOC mechanisms, in contrast to the null model with sets of entirely random events. Secondly, the occurrence of SOC states can deepen our understanding of the nature of collective dynamics and predictability of human behaviour [18,46,47] given the theory of complexity. However, SOC's origin and fundamental role in social systems still need to be better understood, given the complexity of human interactions conveying information or transferring contents (emotional, cognitive) or biological entities. Another striking feature is the occurrence of cycles, from circadian cycles characteristic to the daily activity of humans to large-scale cycles observed, for example, in epidemics spreading or the evolution of collective knowledge. Compatibility of cyclical trends with the critical fluctuations [48–50] is another theoretical question which so far has yet to receive adequate consideration.

In this work, we tackle these questions through an extensive analysis using the representative empirical data which contain online social communications with annotated emotional contents; in particular, the communications taking part throughout an extended period are from the social network MySpace and the social site Diggs. In addition, we used a dataset of infection rate time series from recent epidemics as a real-world example. These publicly available datasets we use were previously collected and described in [22,25,51,52]. While the online social network MySpace can serve as a proxy of a social graph consisting of groups of users from a similar geographical location and often off-line relationships [53], the discussion-driven dynamics on Diggs results in the co-evolution of a bipartite network. In both cases, the respective time series exhibits a prominent circadian cycle characteristic of human activity. However, a detailed analysis of the occurring cycles shows that they are modulated by the collective dynamical behaviours, thus obtaining higher harmonics quantified by a broad multifractal spectrum. The underlying collective dynamics are appropriately described with the scale-invariant avalanches and scaling laws expected in the SOC states. To broaden the view, we have described the relevant properties of human interactions providing minimal parameters necessary to describe such collective dynamic behaviours; they are, for example, used as the agents' properties in the mentioned earlier agent-based modelling approach. We anticipate that these parameters that appear crucial for shaping the collective dynamics are detectable from the underlying empirical data in various social systems. To this end, we demonstrate that similar multi-harmonic cycles also appear in the infection-rate time series.

In Section 2, we briefly survey several features of human dynamics that make a critical difference compared to prototypal model systems of SOC; we specifically focus on the occurrence of evolving cyclical trends in two prominent examples. In Section 3 and Section 4, we analyse the online dynamics data to demonstrate the co-existence of SOC and modified cycles. Section 5 summarises our main findings.

2. Key properties of human dynamics from individual to globalscale

Data that we analyse here are publicly available data of two types. They are represented as time series containing information about human online activity from two social sites over an extended time interval, as explained below, and a dataset of infection-rate fluctuations from recent epidemics. In particular, the data collected from the online social network MySpace and the texts of the corresponding messages are annotated for containing positive and negative emotional contents using the sentiment classifier [54], as described in the original reference [22]. Similarly, the dataset from the social site Diggs is collected and annotated for the positive and negative emotion contents, as described in [25]. Here, we use a subset of the collected data related to the discussion-driven activity on popular posts, termed as *discussion-driven Diggs*. In both cases, the considered time interval comprises three months. Even though the time resolution of data on these sites is high, it was found [22,25] that a more "natural" time unit for the pace of the activity is given by 5-minutes bins. Thus, the online activity time series contain 25,920 data points. The epidemics data are publicly available datasets for Serbia, collected from [51,52]. The corresponding time series contains 1000 data points with a resolution of one day. As shown in the following, the *contents* communicated between human actors plays a vital role in emergent collective behaviour. In particular, the users' activity gets amplified by the positive emotional content in the online social network. Meanwhile, the messages with negative emotions (critique) appear to drive the enhanced activity in the case of indirect user–post–user interactions on Blogs and Digs. On the other hand, the infection-rate fluctuations are induced by the transmission of viruses, which are subject to a given biology and evolution. Before going into a detailed analysis of the above-mentioned time series, we will provide a brief survey of the prominent features of the online social dynamics observed at different scales.

2.1. Online social dynamics reveals the individual actors' properties and emergent collective behaviours

In social psychology, human activity online exhibits regularities that can be related to the personality profiles [20] as well as the communication ways and contents, for example, emotional or cognitive contents and information conveyed via these communications [19]. Analysis of online social dynamics data from different social sites have revealed certain universal patterns of human behaviour and specific networking visualised as a kind of social graph, cf. Fig. 1. Moreover, massive data analysis has allowed extracting statistical features of users, for example, cf. Fig. 2, but without explicitly knowing their personality types; these features provide relevant parameters in the data-related agent-based models. In particular, such analysis of data and agent-based simulations has been performed for the social dynamics in MySpace [22,23], Blogs [24,26], Diggs [25,27,28], and online chats [29], where the emotional contents dominate, and in the collective knowledge creation via Questions-and-Answers [16,30].

Based on the extensive data analysis in the works mentioned above, we can summarise the essential properties of human interactions relevant to shaping the collective dynamics in these online social sites and beyond.

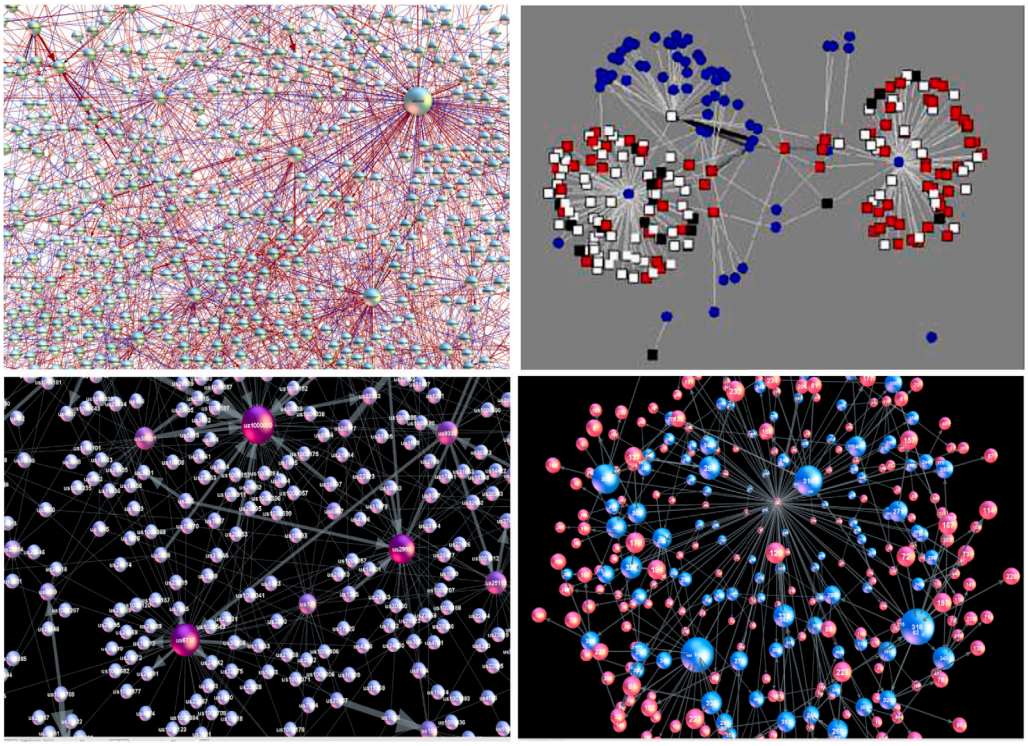

Fig. 1. Zoom-in dialogues structure inside OSN MySpace (top left) with emotional messages shown by colours on edges: positive (red), negative (blue) and neutral (black). Part of the Ubuntu chats layer selected according to the specific type of communications annotated as *No-Answer* (bottom left). Bipartite networks of users (blue nodes) and posts and comments with emotional content (red — positive, black — negative, and white — neutral) related to a popular Blog (top right) and a popular Question (bottom right); large nodes indicate a few very active users. (For interpretation of the references to colour in this figure legend, the reader is referred to the web version of this article.)

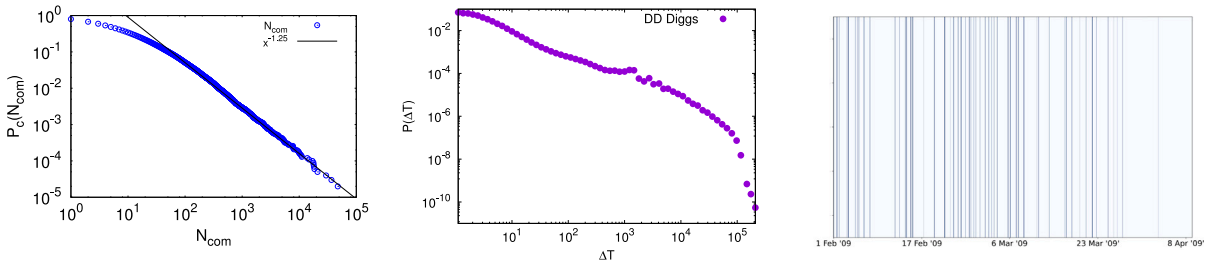

Fig. 2. Histogram of the number of actions per user in the data of popular Blogs, left, delay-time distribution and intervals between successive steps of a particular user in discussion-driven Diggs, middle and right.

- (a) *Driving* by new-users time series, which can be identified in a considered time interval. New arrivals trigger the activity, i.e., by posting a new question, blog, or message, often conditioned by their offline activity.
- (b) *Users inhomogeneity* regarding the activity level and preferences towards specific contents (information, emotional and cognitive contents) conveyed via communications; temporal fractal patterns of the user's activity with delays. These features lead to the activity distribution and a delay-time distribution with power-law tails, cf. Fig. 2.
- (c) *Networks co-evolving* with the users' activity, i.e., in specific elements or global structure, thus providing feedback on the dynamics; the dynamically changing structure manifests itself in the varying activity level of nodes, the use of particular links, and emergent communities and network layers related to specific features of communicated contents; see Fig. 1 for four prototypal examples.
- (d) *Scale-invariant avalanches of activity* occur as cascades of events with power-law probability distributions; the events can be selected according to a given searched cognitive content or the emotion of a given valence. Consequently, the related avalanches may appear to have different statistical features. The scale-invariance extends to the power spectra of the activity time series, exemplifying the long-range temporal correlations in a given frequency range. These properties are often recognised as signatures of self-organised criticality, as discussed below. Another possible origin of scale invariance in such dynamical systems could be related to the dynamical phase transitions, e.g., by changing a critical parameter.
- (e) *Cyclical trends* starting from the apparent circadian cycles of humans to the emergent large irregular cycles, e.g., such as seen in the epidemics spreading, are profound features of collective human behaviours. As we show in this work, these cycles can get modulated via collective dynamics, attaining multi-fractal characteristics, in analogy to physical systems in the dynamical critical states [48–50].

The features marked as (a) and (b) appear as minimal parameters for the appropriate agent-based models [] that can recover the global quality of that dataset and predict its further developments, given the range of parameter variations. They can be extracted from the related

empirical dataset. Fig. 2 shows two such properties, in particular, the power-law distribution of the number of actions per user (within a given time interval captured by the dataset) and a fractal pattern of individual user actions in time.

Networking via communications is another remarkable feature of social dynamics; the underlying networks of different types and graph properties that evolve with the dynamics can be extracted from the empirical data. Some prototypal examples are shown in Fig. 1. We can differentiate these emergent networks according to two principles, i.e., regarding (un)mediated user communications, on one side and the presence (absence) of a collective endeavour on the other. In the examples shown, the indirect user–post–user communications on Blogs and `Diggs` are best characterised as bipartite graphs. Meanwhile, the direct user–user communications occurring in the `MySpace` and the Ubuntu chat networks are represented by mono-partite graphs. `MySpace` starts as a social graph (mostly containing offline-associated individuals); meanwhile, the network is formed via Ubuntu chats beginning from a small initial group of users, adding new users who seek help to solve a specific programming problem. Many users remain within a growing community for a long time helping new arrivals solve their problems. Supported by this cooperative behaviour, the graph that emerges through these long-term links was shown to have a "social-graph" architecture, according to the social-hypothesis criteria, see detailed analysis in Ref. [55]. Similarly, the social endeavour behind creating collective knowledge, studied in [30], even though involving indirect interactions, leads to the emergence of an explicit-knowledge network of contents (annotated by mathematical tags), which has logical structure [56]. Conversely, using the existing links by individual "players" in `MySpace` causes the evolution to deviate from the social graph structure, as shown in Ref. [22]. The dominance of positive emotional valence in the exchanged messages leads to a structure similar to that found in online games [57]. In the mentioned bipartite networks, conversely, negative-emotion communications prevail, thus determining the evolution of communities of the involved users. The network's evolution has feedback to the dynamics, thus strengthening the collective effects.

The properties marked as (d) and (e) are the collective dynamics effects emerging at a larger scale; they can be studied from the time series data, as shown in the following section. Another emergent feature we are concerned with here is the occurrence of cycles in collective dynamics. The two striking examples demonstrate it based on the analysis of the empirical data.

2.2. From circadian cycles to emergent multiharmonic trends in social dynamics

As mentioned in the Introduction, two prominent examples of emergent cyclical trends in social systems are analysed here using publicly available empirical data. In particular, they are shown in Fig. 3: (i) the infection-rate fluctuations from recent epidemics (data from [51,52] are for Serbia, data resolution is one day, the length of 1000 days); (ii) the online communication dataset collected from the discussion-driven `Diggs` (data collected and described in [25]; data resolution is 5 minutes bins, the length of three months). In Section 4, we show that similar cycles emerge in the SOC state analysed in the data from `MySpace` of the same length.

We use the local adaptive detrending algorithm [22,58] to determine cyclical trends in these datasets. Specifically, we adapt the method of overlapping time intervals, based on the original work in [58] for sunspot cycles, and used in [22,48,49] for different types of time series in physical and social systems. In this method, the considered time series is divided into segments of the length $2m+1$, which overlap over $m+1$ points; the segments are enumerated as $k = 0, 1, 2, \cdots k_{max} = T_{max}/m - 1$, where T_{max} stands for the length of time series. Then, the polynomial fit $y^{(k)}(mk+\ell)$ in each segment are determined over $\ell = 0, 1, 2, \cdots 2m$ points and used to determine local trends. Specifically, for $0 < k < k_{max}$, the trend $y_c(mk+i)$ over the overlapping points is determined as $y_c(mk+i) = \frac{i}{m} y^{(k+1)}(mk+i) + \frac{m-i}{m} y^{(k)}(m(k+1)+i)$, where $i = 0, 1, 2 \cdots m$ combining the contribution in segment k with the one in segment $k+1$. Notably, in the overlapped region, the corresponding polynomial contribution decreases linearly with the distance from the segment's centre. Meanwhile, in the initial $m+1$ points in $k = 0$ and the final $m+1$ points in $k = k_{max}$ segments, and the trend coincides with the actual polynomial fit. The parameter m is adjusted for each considered time series; meanwhile, the linear interpolation suffices for the studied time series.

From the discussion-driven `Diggs` data, we use the subset with the comments that contain negative emotional valence and determine two types of cycles in it. These time series with the resulting cycles are shown in Fig. 3a. The rationale behind this selection is that as a detailed analysis in Ref. [25] revealed, the post's popularity correlates with the excess negative emotion (see also other studies [27,28] with post-mediated interactions among users). Moreover, it was shown that the users networking over such posts led to the emergence of communities, whose size oscillates with the fluctuations of the 'negative change' of the related posts (see Fig. 2 in [25] for details). As Fig. 3a shows, the number of comments carrying negative emotion (black line) varies in time with a prominent daily cycle (indicated by the red line), which can be related to the circadian (day–night) cycle of the users' activity. Furthermore, we find a large cycle on the approximate weekly scale, indicated by the pale colour in this figure. Interestingly, the users' community size, computed from the network mapped on each consecutive day in [25], shown by the blue line with crosses in Fig. 3a, fluctuates in time per the observed weekly cycle. We show the largest community for demonstration, but the other communities were found to show a similar pattern [25].

Further analysis of these cycles shows that they are modulated, attaining different harmonics due to underlying collective dynamics. These temporal fluctuations with many harmonics are compatible with a broad singularity spectrum in the appropriate multi-fractal analysis, as described below in Section 4. The corresponding singularity spectra of both daily and weekly cycles of these time series are shown in the inset of Fig. 3a. In the case of the infection cycles, shown in Fig. 3b, the trend (red line) appears with broader irregular cycles, resulting in the interplay of a more complex bio-social stochastic process [59,60]. Apart from the interactions taking part in real space, where human mobility greatly contributes [61], the virus biology, transmissibility and virulence make new essential ingredients. Consequently, the elementary cycle during which an infected individual can infect others is enlarged; for example, it extends over 10–14 days in the case of SARS-CoV-2 epidemics. All these elements combine with the applied social measures into complex bio-social processes, resulting in the emergent infection cycles, as the example in Fig. 3b. The related multi-fractal analysis also leads to a broad singularity spectrum of the observed cycle, shown in the inset to Fig. 3b. In both cases, the singularity spectra are non-symmetrical, with the enhanced right side corresponding to small-size fluctuations. This feature seems markedly characteristic of collective social dynamics; see also Section 4.

3. Self-organised criticality of emotion-driven collective behaviours in OSN

In this section, we analyse time series of emotional dialogues in `MySpace` focusing on the occurrence of avalanches of events and their scaling properties that are compatible with the SOC states. In particular, in our dataset, we consider the overall activity time series and separated parts of the activity reflecting the positive and negative emotional communication, respectively. Moreover, as explained above, we analyse the driving "force" of the activity–new-user time series. As described above, these time series are from Ref. [22], the corresponding time interval is three months with the resolution of 5 minutes bins. The representative segments of these time series are given in Fig. 4a,b;

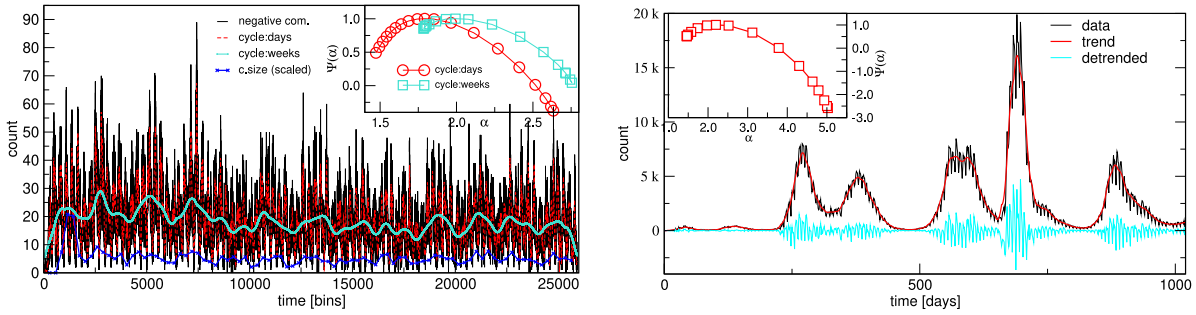

Fig. 3. Left: Circadian cycles and emergent community activity cycles in the emotion-driven discussions on popular Diggs (data from [25]); Right: The number of daily infected individuals exhibiting cyclical trend (Covid-19 data from [51,52]). Insets: The corresponding singularity spectra obtained by multi-fractal analysis suggest the presence of higher harmonics in cyclical trends. (For interpretation of the references to colour in this figure legend, the reader is referred to the web version of this article.)

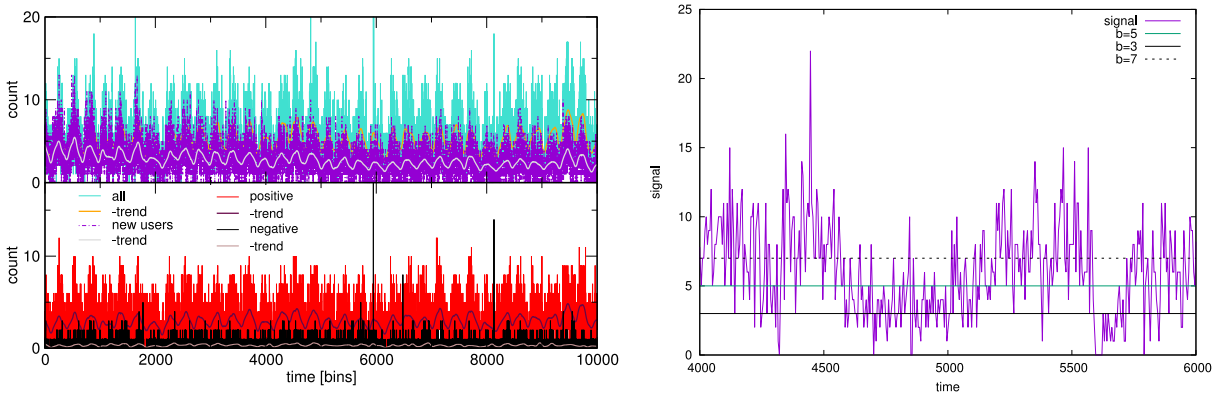

Fig. 4. From MySpace data, time series of (a) new users and all messages and (b) positive and negative emotional messages with daily cyclical trends, as indicated in the legend. (c) A segment of time series with different threshold values b; a part of the signal above the threshold between two consecutive drops to the threshold line defines an avalanche. Conversely, the distance between successive avalanches δT is identified as segments of a threshold line above which there is no signal. (For interpretation of the references to colour in this figure legend, the reader is referred to the web version of this article.)

as this figure shows, apart from the bursts of events, these time series exhibit prominent daily cycles. Moreover, these cycles are introduced via the new-user time series (pink line in panel (a)), which busts the whole activity in this OSN. The properties of cycles will be analysed in Section 2.2; meanwhile, here, we focus on the burstiness of events, which determines avalanches and their specific scale-invariant features in the presence of these cyclical trends.

Given the definition of avalanches in the prototypal SPA models [], here we determine them from time series, following the procedure developed for physical systems, see, e.g., Ref. [62]. For a given time series (e.g., with data points c_t), an avalanche is determined as a part of the signal *above a threshold line* between two consecutive drops to the baseline. More precisely, the avalanche size S is given by the sum $S = \sum_{t_b}^{t_e} c_t$, and the avalanche duration $T = t_e - t_b$, where t_b and t_e are considered two consecutive intersections of the signal and the baseline. See Fig. 4c for illustration. The level of the baseline is determined, for example, in the experimental signals, in such a way as to eliminate additional noise, considered as not originating from the studied process. Moreover, increasing the baseline level, which impacts the avalanche measures, tests the resulting avalanche distributions' self-similarity and determines the inter-avalanche distances; see a recent study in [63] and references there.

The most striking feature of SOC states is self-similarity or the absence of the characteristic scale of avalanches, which is compatible with a power-law decay of the corresponding distributions of their size $X \equiv S$ and duration $X \equiv T$ for a range of values before a cut-off. Specifically,

$$P(X) = P_0 X^{-\tau_X} e^{-(X/X_0)^{\sigma_X}} , \tag{1}$$

with the corresponding scaling exponents τ_S, τ_T, and a stretched-exponential cut-off, described with the exponent σ. Given that different avalanche properties steam from the same nonlinear dynamics, their characteristics, e.g., the size and duration, are statistically related. Specifically, selecting all avalanches of a given duration, their average size scales with the duration T is given as $\langle s \rangle_T \sim T^{\gamma_{ST}}$, and the exponent is expressed as

$$\gamma_{ST} = (\tau_T - 1)/(\tau_s - 1). \tag{2}$$

Applying this methodology separately to the time series of the number of all messages and the number of messages with positive/negative emotion valence, we obtain the corresponding distributions $P(S)$ of the avalanche sizes and $P(T)$ avalanche durations. The analysed data are from the dialogues network of 2-months time depth and the zero thresholds. The results for the cumulative distributions are shown in Fig. 5. Apart from the coalescence of simultaneous events, that may increase the occurrence of large avalanches, the distributions of avalanche sizes and durations exhibit a power-law over two orders of magnitude before the cut-off, according to the expression (1), where $X > S$ or $X > T$, stands for the cumulative distribution of size and the duration of avalanches, respectively. The fit curves according to the expression (1) are also shown with the corresponding distributions in Fig. 5. In the size distribution of all avalanches, a stretching exponent $\sigma = 3$ is needed to fit the whole curve. The inset to Fig. 5 shows that the geometry of all three types of avalanches detected satisfies the expected scaling of Eq. (2). Fitted values of the exponents for all distributions are summarised in Table 1, where we also show the corresponding exponents of the power spectrum and standard-deviation fluctuations (Hurst) exponent of these respective time series.

Among the emotional bursts, the avalanches with positive emotional messages prevail. The avalanches of emotional messages are shorter than those of all messages. This feature suggests that, apart from the

Table 1
Fitted values of the scaling exponents for different quantities and types of messages.

Quantity/ Type of messages	All	Positive	Negative
Power spectrum	$\phi^a = 0.59 \pm 0.08$	$\phi^+ = 0.55 \pm 0.08$	$\phi^- = 0.15 \pm 0.06$
Hurst exponent	$H^a = 0.750 \pm 0.03$	$H^+ = 0.698 \pm 0.02$	$H^- = 0.528 \pm 0.03$
Avalanche size	$\tau_s^a - 1 = 0.442 \pm 0.007$	$\tau_s^+ - 1 = 0.623 \pm 0.003$	$\tau_s^- - 1 = 0.31 \pm 0.35$
Avalanche duration	$\tau_T^a - 1 = 0.59 \pm 0.01$	$\tau_T^+ - 1 = 0.83 \pm 0.01$	$\tau_T^- - 1 = 0.66 \pm 0.17$
Avalanche geometry	$\gamma_{ST}^a = 1.32 \pm 0.06$	$\gamma_{ST}^+ = 1.21 \pm 0.05$	$\gamma_{ST}^- = 1.14 \pm 0.07$

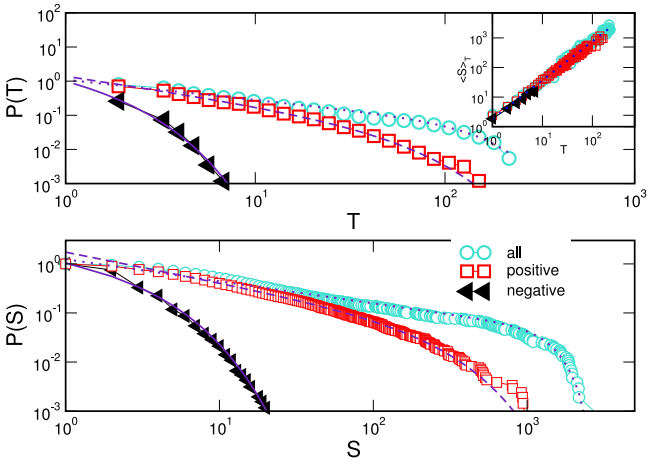

Fig. 5. Cumulative distributions of the size S and duration T of avalanches extracted from MySpace emotional dialogues data. Inset shows the scaling of the average size of the related duration, according to Eq. (2).

network size, another characteristic length occurs, i.e., $s_0 \sim 242 \pm 4$ for the size and $T_0 = 44.8 \pm 1.6$ for the duration of positive emotion avalanches. On the other hand, the negative valence avalanches are very short; the fitting parameter is $s_0 = 3.2 \pm 0.5$, $T_0 = 1.1 \pm 0.1$ with practically no scaling region. Compared with the avalanches of all messages, where much more significant cut-offs $s_0 = 1135 \pm 199$ and $T_0 = 139 \pm 20$ are found, the emotion-carrying events are sub-critical. The finite cut-off lengths can be related to different opposing mechanisms that stop the propagation of the emotional messages of a given polarity.

As Fig. 5 shows, the cut-off dominated distributions are obtained for all avalanche types apart from a variable range with the power-law decay. The relevance of cut-off size (and form) for the SOC states is captured by finite-size scaling analysis. The rationale is that the avalanches in the SOC states of model systems are limited only by the system size due to the absence of any other relevant parameter. Therefore, a scaling form $P(X, L) = X^{-\tau_X} \mathcal{P}(X/\xi_X, X/L^{D_X})$ would apply, where D_X stands for the respective fractal dimension of the considered avalanche distribution. As a good example, see [64] for the finite-size scaling analysis of Barkhausen avalanches.

However, this scaling is challenging to implement for the avalanches occurring on networks, as a potential linear dimension plays a different role. In a more general context, not a single fractal dimension can be assigned to the avalanche propagation. Instead, a multifractal scaling compatible with a spectrum of (local) fractal dimensions is more appropriate. Specifically the following multi-fractal scaling form [65–67], for example, for the avalanche size distribution $P(S, L)$:

$$P(S, L) = \left(L/L_0\right)^{\Phi(\epsilon)}, \epsilon = \frac{log(S/S_0)}{log(L/L_0)}, \tag{3}$$

which is compatible with the spectrum $\Phi(\epsilon)$ of the fractal dimensions ϵ. In the following, we show that this form applies to the avalanches determined by the increasing threshold b, which we determine from MySpace messages collected at a three-months depth dataset; they are shown in Fig. 6. Here, the effective "distance" L varies with the threshold b as $L = L(b) \sim b^{-1/\lambda}$, and λ, L_0 and S_0 are the fit parameters determined from the scaling collapse; see bottom right panel in Fig. 6. It is also important to note that the avalanches determined at different thresholds have power-law segments above a particular scale. More precisely, huge avalanches responsible for the pronounced stretched exponential cut-off as in Fig. 5, are now absent. Consequently, these distributions can be fitted by Tsallis' q-exponential [68] form

$$P(S) = a\left[1 - (1-q)\frac{S}{s_0}\right]^{1/1-q}; \tag{4}$$

The estimated values of the non-extensivity parameter q are shown in the figure legends, cf. Fig. 6, for the case when $b = 1$. In this case, the power-law range extends for almost two decades for the size and duration of avalanches, allowing appropriate fitting. Note that the corresponding scaling exponent $\tau = 1/(q-1)$ estimated from the values shown in panels (a) and (b) are $\tau_T \sim 1.92$ and $\tau_S = 1.67$ are close to the MF exponents of SOC. As stated above, these avalanches obtained for different threshold heights obey multifractal scaling, according to the expression (3). It is demonstrated in panel (d) for the avalanche sizes distributions shown in panel (b) of Fig. 6. In this case, the effective linear dimension in the expression (3) is tunned by increasing threshold b as $L \sim b^{-1/\lambda}$ where the numerical values are estimated as $\lambda = 0.31(5)$ corresponding to the best fit, meanwhile, $L_0 = 1$ and S_0 is in the range from 13 to 18, cf. Fig. 6d. In addition, the distributions of the inter-avalanche times δT are determined for different thresholds; they also show an apparent power-law decay, according to Eq. (4), as shown in Fig. 6c. The corresponding q-values are indicated in the legend.

To conclude this section, the occurrence of cycles in the studied time series, cf. Fig. 3, interferes with the avalanche distributions determined from them. In particular, for the zero thresholds, the circadian cycle influences the count of large avalanches, thus affecting the cut-off length of the avalanche distributions. On the other hand, with the elevated threshold, the avalanches are determined from the bursts of events within each given cycle. However, the presence of a cyclical trend impacts the distribution of these avalanches such that they are more compatible with the q-exponential functional form and a multi-fractal scaling, which allows a spectrum of fractal exponents (different fractal exponent for each segment type).

4. Multiscale cycles coexisting with emotion-driven collective dynamics

In this section, we detail the cyclical trends in the time series shown in Fig. 4a,b, representing the emotion-driven dialogues in MySpace. As it is shown below, they are not regular cycles but exhibit additional harmonics, which will be revealed through the multifractal analysis.

To analyse the multi-scale fluctuations [69] of time series data, $\{c_t\}$, we use the detrended multifractal analysis, see [70,71] and references there. The time series profile $Y(i) = \sum_{k=1}^{i}(c_k - \langle c_k \rangle)$ is divided the into $K = int(T_{max}/n)$ non-overlapping segments of the length n, where T_{max} stands for the length of time series. The local trend $y_\mu(i)$ is found at each segment $\mu = 1, 2, \cdots K$, and the standard deviation around it is determined as $F^2(\mu, n) = \frac{1}{n}\sum_{i=1}^{n}[Y((\mu-1)n+i) - y_\mu(i)]^2$. The procedure is repeated starting from the end of the signal, resulting in $2K$ segments over which the fluctuation function is to be averaged. The rth order

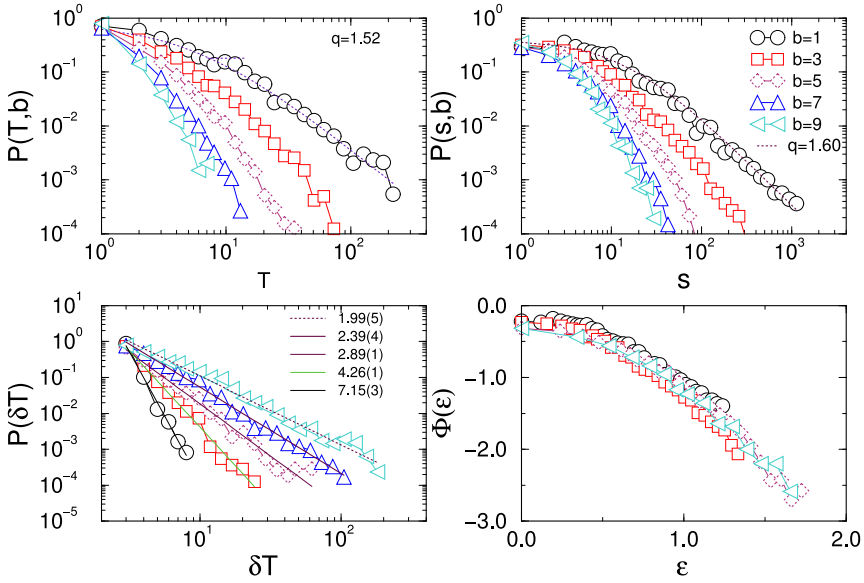

Fig. 6. Distributions of avalanche durations (a) and sizes (b) for varied threshold b and the distribution of inter-avalanche distances for different thresholds (c). Panel (d) shows the multi-fractal scaling of the size distributions from panel (b).

fluctuation function $F_r(n)$ for varying segment length n is determined as

$$F_r(n) = \left\{ \frac{1}{1K} \sum_{\mu=1}^{2K} \left[F^2(\mu, n)\right]^{r/2} \right\}^{1/r} \sim n^{H_r} , \tag{5}$$

and its scaling properties investigated for a range of parameters r. Thus, the generalised Hurst exponent H_r is determined as the slope of straight line segments in the log–log plot of the fluctuation function for each r value. A range of negative and positive values for the amplification parameter r are considered, corresponding to the small and large fluctuations. In this context, the standard deviation function corresponds to $r = 2$, and the exponent H_2 is the standard Hurst exponent. For a *mono-fractal* time series $H_r \approx H_2$ for all values of r; meanwhile, a spectrum of the generalised exponents H_r is observed for a multifractal signal.

Having determined the generalised Hurst exponent H_r as a function of r, a link to the exponentτ_r, related to the box probability measure in the partition function methods can be done [72] given the scaling relation $\tau_r = rH_r - 1$. This relation provides another interpretation of the observed multi-fractal features in terms of the *singularity spectrum* $\Psi(\alpha)$, which is determined via Legendre transform of τ_r as $\Psi(\alpha) = r\alpha - \tau_r$. Different α values in a broad spectrum $\Psi(\alpha)$ suggest that the underlying time series exhibits various power-law singularities at different data points, according to [72,73]. For a mono-fractal, it reduces to a single point.

A segment of the time series (all messages) from Fig. 4a is shown in Fig. 7 left panel; it exhibits the above-mentioned daily cycle, but also another (approximately weekly) cycle trend. The fluctuations around the daily cycle trend are also shown (detrended signal). In the right panel, the original and detrended signal's power spectra and daily and weekly trends are shown. The power-spectrum decay at high frequencies is compatible with an exponent, which is close to two, for both cyclical trends in their respective range of frequencies (times shorter than the observed cycle length). However, they follow another functional dependence in the region of lower frequencies (longer times). The respective multi-fractal analysis reveals that they contain higher harmonics, which results in broad singularity spectra, as shown in Fig. 8.

As Fig. 8 shows, the fluctuation function $F_r(n)$ vs n for daily and weekly trends exhibits a scaling region where the lines for different r identify other Hurst exponent; the straight lines indicate these regions. Meanwhile, they are monofractals with $H_2 = 1.94(2)$ in the area for smaller n values. Consequently, the Hurst exponents H_r determined in these multifractal scaling regions lead to singularity spectra, shown in the lower inset (colour-matching, open circles). Notably, the spectrum of the daily-cycle fluctuations exhibits enhanced small-fluctuations side (large α values). A similar feature is found in such cycles of the emotion-contents time series and new-user time series, cf. legend in the lower inset of Fig. 8. We can conclude that, in this OSN, such fluctuations are primarily induced by the driving signal–new-user time series! On the other hand, the emergent cycle (at the weekly scale) has a different scaling region and spectrum, which is more symmetrical or slightly inclined towards large-fluctuations exponents (small α). We recall that, in the above Fig. 3 (left), an emergent cycle at a weekly scale is driven by the dynamical formation of groups in discussion-driven `Diggs` with a negative emotional content; however, its singularity spectrum is shifted towards larger α values, indicating a different underlying dynamics of bipartite graphs compared to the fixed social network studied here.

5. Conclusions and discussion

We have studied signatures of self-organised criticality using high-resolution data collected from OSN's dialogues with emotional contents. Our aim was to gain a more profound understanding of the role of SOC states in social dynamics. This task, however, is challenged by ubiquitous cycles in social systems. In contrast to fractal bursts of events and avalanches that characterise SOC behaviours, cycles tend to make the systems' evolution more 'regular' and predictable. The natural day–night activity variation (circadian cycle) of individuals may be seen as an origin of cyclical fluctuations in collective human behaviours; its mixing-up with stochastic processes that involve human interactions of a different kind (exchange of information, emotion, knowledge, or even biological agents, e.g., in the epidemics) leads to the emergence of the cyclical trends at different time scales.

Our systematic study of both cycles and avalanches shows that the SOC coexists with emergent multiscale cycles in certain dynamical regimes. Moreover, their mutual influence, quantified by appropriate multifractal measures, appears as a noteworthy feature of the collective social dynamics. In particular,

- Cycles get modified, and new cycles emerge in the SOC states by collective dynamics such that they attain higher harmonics,

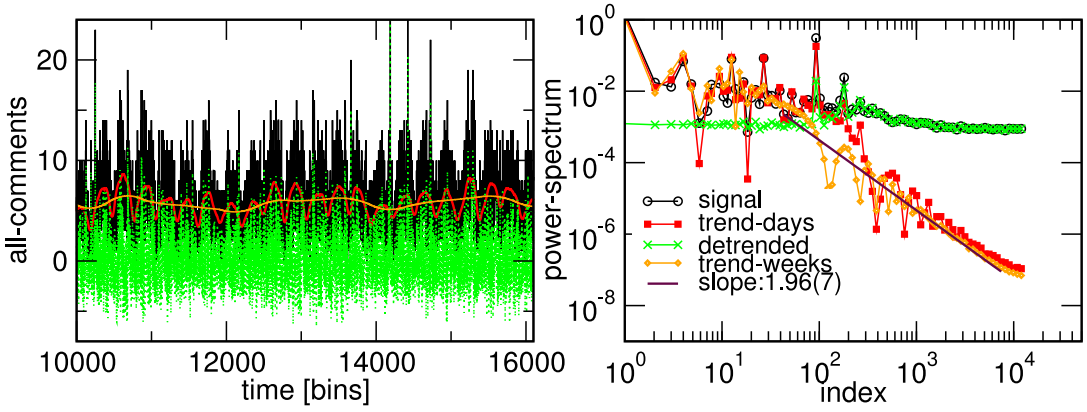

Fig. 7. Left panel: MySpace time series for the number of all messages (black line) showing trends as daily cycles (red line) and weekly cycles (orange). The detrended signal around the daily cycle is also shown (green). Their corresponding power spectra are given in the right panel. (For interpretation of the references to colour in this figure legend, the reader is referred to the web version of this article.)

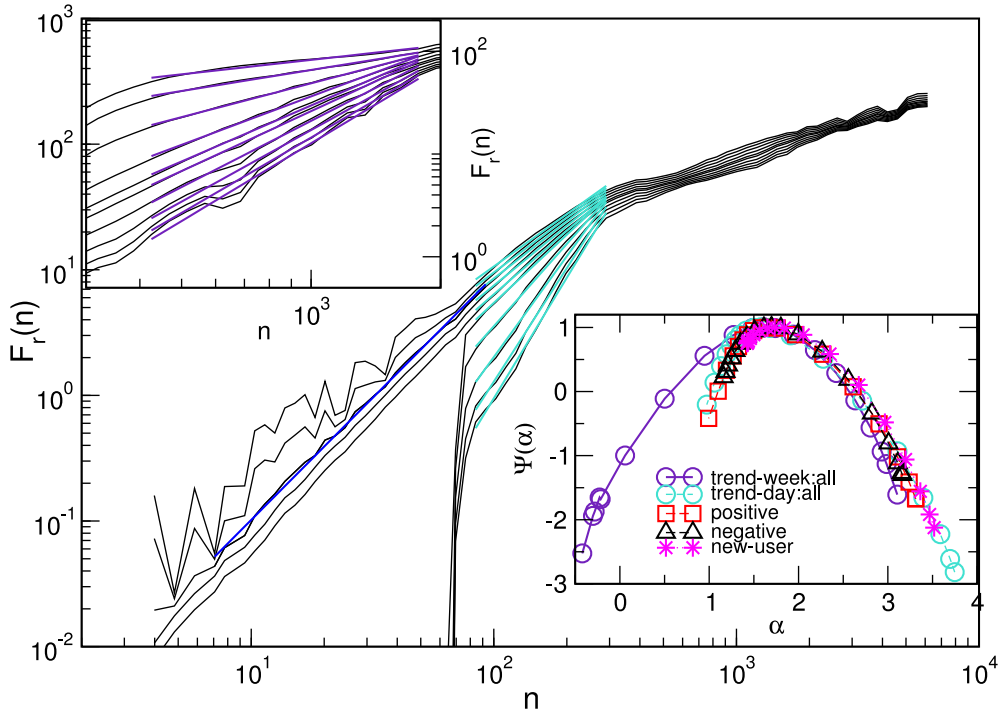

Fig. 8. Fluctuation function $F_r(n)$ vs time interval n of the daily (main) and weekly trend (top inset) of the MySpace dialogues time series; their singularity spectra (bottom inset); also shown are the spectra for the daily cycles of the time series containing positive/negative emotional messages and the trend of new-users time series, as indicated in the legend.

resulting in broad singularity spectra. Similar modulations of the cyclical trends are observed and quantified by their multifractal features in different online and offline social dynamics data.

- The bursting events inside the cycle's range are adequately captured by avalanches with scale-invariant distributions and scaling relations characteristic to SOC states. In contrast to the typical scaling of avalanches in model SOC systems, the social-dynamics avalanches in the presence of prominent cycles are better described by Tsallis distribution and multifractal scaling, analogous to the ones in earthquake dynamics. This observation also applies to the avalanches in the social endeavour of collective knowledge creation [30]. Similarly, the inter-avalanche time exhibits scale invariance, supporting this analogy.
- The multiscale fluctuations of cycles correlate with the emergence of groups of users aggregated about specific posts; these groups can be identified as topological communities from the network's mapping over time; the underlying contents communicated through the network play an important role (e.g., negative emotion in the related posts, in the studied example).

This dynamical regime, here revealed in the online dynamics with emotional dialogues, is characterised by fast communications (relative to the elementary circadian cycle). In addition, the prominent user heterogeneity in content-based communications introduces a broad range of obstacles to propagating a given (emotional, cognitive) content. Conversely, a cycles-dominated dynamical regime exists; the studied case of infection-rate Covid-19 data for the new virus type exemplifies it. As a rule, these cycles are more extensive, originating from different bio-social stochastic processes and an elementary cycle that extends over several days. These cyclical trends are irregular with a broad singularity spectrum, suggesting an interplay with collective social dynamics. However, at the time scale that the data are recorded, the nature of fluctuations within a cycle means that the long-range

temporal correlations are washed out. These facts indicate that, apart from the dominant biological factors, different social mechanisms are at work; some ad-hoc groups of various sizes emerge in space and dissolve on a smaller time scale than the infection spreading is recorded. A deeper understanding of the appearance of such cycles requires the appropriate agent-based modelling, which appropriately incorporates the relevant biological factors and multiple time scales; some recent attempts can be found in [59,60,74].

In conclusion, our study unveils two regimes in social dynamics with a distinct interplay of cyclical trends and collective dynamics. The contents communicated via social interactions play an essential role. The results with high-resolution data shed new light on the coexistence of self-organised criticality and social cycles. On one side, the nature of avalanches is altered in the presence of cycles. Meanwhile, the cycles attain multiple harmonics due to the correlated fluctuations behind these avalanches, thus making the dynamical states less predictable and more robust to various perturbations. The coexistence of multiscale cycles and self-organised criticality, quantified through the multifractal analysis, thus can be seen as a notable feature of the high-resolution social dynamics.

Declaration of competing interest

The authors declare that they have no known competing financial interests or personal relationships that could have appeared to influence the work reported in this paper.

Data availability

Data will be made available on request.

Acknowledgements

B.T. acknowledges the financial support from the Slovenian Research Agency (research code funding number P1-0044). R.M. is grateful to the NSERC, Canada and the CRC program for their support. M.M.D. acknowledge funding provided by the Institute of Physics Belgrade, through the grant by the Ministry of Science, Technological Development and Innovation of the Republic of Serbia.

References

[1] Bak P, Tang C, Wiesenfeld K. Self-organized criticality: An explanation of 1/f noise. Phys Rev Lett 1987;59:381–4.
[2] Dhar D. Self-organized critical state of sandpile automaton models. Phys Rev Lett 1990;64(14):1613–6.
[3] Jensen HJ. Self-organized criticality: emergent complex behavior in physical and biological systems. (Cambridge lecture notes in physics), Cambridge University Press; 1998.
[4] Aschwanden MJ. Self-organized criticality systems. Berlin Warsaw: Open Academic Press; 2013.
[5] Marković D, Gros C. Power laws and self-organized criticality in theory and nature. Phys Rep 2014;536(2):41–74.
[6] Watkins NW, Pruessner G, Chapman SC, Crosby NB, Jensen HJ. 25 Years of self-organized criticality: Concepts and controversies. Space Sci Rev 2016;198(1–4).
[7] Plenz D, Niebur E. Criticality in neural systems. Wiley-VCH Verlag GmbH & Co. KGaA; 2014.
[8] Walter N, Hinterberger T. Self-organized criticality as a framework for consciousness: A review study. Front Psychol 2020;13:911620.
[9] Smyth WD, Nash JD, Moum JN. Self-organized criticality in geophysical turbulence. Sci Rep 2019;9.
[10] Vidiella B, Guillamon A, Sardanyés J, Maull V, Pla J, Conde N, et al. Engineering self-organized criticality in living cells. Nature Commun 2021;12(1).
[11] Rosenfeld S. Global consensus theorem and self-organized criticality: Unifying principles for understanding self-organization, swarm intelligence and mechanisms of carcinogenesis. Gene Regul Syst Biol 2013;7. GRSB.S10885, PMID: 23471309.
[12] Tsuchiya M, Giuliani A, Hashimoto M, Erenpreisa J, Yoshikawa K. Emergent self-organized criticality in gene expression dynamics: Temporal development of global phase transition revealed in a cancer cell line. PLOS ONE 2015;10:1–33.
[13] Tadić B, Malnik R. Self-organised critical dynamics as a key to fundamental features of complexity in physical, biological, and social networks. Dynamics 2021;1(2):181–97.
[14] McAteer R, Aschwanden M, Dimitropoulou M, Georgoulis M, Pruessner G, Morales L, et al. 25 Years of self-organized criticality: Numerical detection methods. Space Sci Rev 2016;198(1–4).
[15] Corominas-Murtra B, Hanel R, Thurner S. Understanding scaling through history-dependent processes with collapsing sample space. Proc Natl Acad Sci 2015;112(17):5348–53.
[16] Mitrović Dankulov M, Tadić B, Melnik R. The dynamics of meaningful social interactions and the emergence of collective knowledge. Sci Rep 2015;5.
[17] Font-Clos F, Boleda G, Corral Á. A scaling law beyond Zipf's law and its relation to heaps' law. New J Phys 2013;15(9):093033.
[18] Bellomo N, Gibelli L, Quaini A, Reali A. Towards a mathematical theory of behavioral human crowds. Math Models Methods Appl Sci 2022;32(02):321–58.
[19] Holyst JA, editor. Cyberemotions: collective emotions in cyberspace. Springer International Publishing; 2017.
[20] Amichai-Hamburger Y, Vinitzky G. Social network use and personality. Comput Hum Behav 2010;26(6):1289–95, Online Interactivity: Role of Technology in Behavior Change.
[21] Ahn Y-Y, Han S, Kwak H, Moon S, Jeong H. Analysis of topological characteristics of huge online social networking services. In: Proceedings of the 16th international conference on world wide web. 2012, p. 835–44.
[22] Šuvakov M, Mitrović M, Gligorijević V, Tadić B. How the online social networks are used: Dialogs-based structure of myspace. J R Soc Interface 2012;10:20120819.
[23] Tadić B, Šuvakov M, Garcia D, Schweitzer F. Agent-based simulations of emotional dialogs in the online social network myspace. Cham: Springer International Publishing; 2017, p. 207–29.
[24] Mitrović M, Paltoglou G, Tadić B. Networks and emotion-driven user communities at popular blogs. Eur Phys J B 2010;77(4).
[25] Mitrović M, Paltoglou G, Tadić B. Quantitative analysis of bloggers' collective behavior powered by emotions. J Stat Mech Theory Exp 2011;2011(02):P02005.
[26] Mitrović M, Tadić B. Dynamics of bloggers' communities: Bipartite networks from empirical data and agent-based modeling. Physica A 2012;391(21):5264–78.
[27] Mitrović M, Tadić B. Emergence and structure of cybercommunities. Boston, MA: Springer US; 2012, p. 209–27.
[28] Tadić B, Gligorijević V, Mitrović M, Šuvakov M. Co-evolutionary mechanisms of emotional bursts in online social dynamics and networks. Entropy 2013;15(12):5084–120.
[29] Tadić B, Šuvakov M. Can human-like bots control collective mood: Agent-based simulations of online chats. J Stat Mech Theory Exp 2013;2013(10):P10014.
[30] Tadić B, Mitrović Dankulov M, Melnik R. Mechanisms of self-organized criticality in social processes of knowledge creation. Phys Rev E 2017;96:032307.
[31] Dmitriev A, Dmitriev V, Balybin S. Self-organized criticality on Twitter: Phenomenological theory and empirical investigation based on data analysis results. Complexity 2019;2019.
[32] Dmitriev A, Dmitriev V. Identification of self-organized critical state on twitter based on the retweets' time series analysis. Complexity 2021;2021.
[33] Batty M, Xie Y. Self-organized criticality and urban development. Discrete Dyn Nat Soc 1999;3.
[34] Chen Y, Zhou Y. Scaling laws and indicators of self-organized criticality in urban systems. Chais Solitons Fractals 2006;35:85–98.
[35] Zhukov DS. Online rebellion: Self-organized criticality of contemporary protest movements. SAGE Open 2022;15(2):63–77.
[36] Tebaldi C. Self-organized criticality in economic fluctuations: The age of maturity. Front Phys 2021;8.
[37] Philippe P. Epidemiology and self-organized critical systems: An analysis in waiting times and disease heterogeneity. Nonlinear Dyn Psychol Life Sci 2000;4(4).
[38] Arroyo D, Tonello L, Giacobbi L, Pettenon A, Scuotto A, Cocchi M, et al. Crisis behavior in autism spectrum disorders: A self-organized criticality approach, vol. 2018. 2018.
[39] Brunk GG. Self-organized criticality: A new theory of political behaviour and some of its implications. Br J Polit Sci 2001;31(2):427–45.
[40] Zhukov DS, Kanishchev VV, Lyman SK. How the theory of self-organized criticality explains punctuated equilibrium in social systems. SAGE open 2020. 7872/241450824049023039523 43.
[41] Kron T, Grund T. Society as a self-organized critical system. Cybern Hum Knowing 2009;16(1–2):65–82.
[42] Brunk GG. Why do societies collapse?: A theory based on self-organized criticality. J Theoret Polit 2002;14(2):195–230.
[43] Tang X, Ye H. Metaphorical language change is self-organized criticality. In: Corpus linguistics and linguistic theory. 2022.
[44] Manna SS, Biswas S, Chakrabarti BK. Near universal values of social inequality indices in self-organized critical models. Physica A 2022;596:127121.
[45] Zhukov DS, Kanishchev VV, Lyman SK. Application of the theory of self-organized criticality to the investigation of historical processes. SAGE Open 2016;6(4):2158244016683216.

[46] Ramos RT, Sassi RB, Piqueira JRC. Self-organized criticality and the predictability of human behavior. New Ideas Psychol 2011;29(1):38–48.
[47] Degond P. Mathematical models of collective dynamics and self-organization. 2018, p. 1–20, ArXiv:1809.02808v1.
[48] Tadić B. Cyclical trends of network load fluctuations in traffic jamming. Dynamics 2022;2(4):449–61.
[49] Mijatović S, Graovac S, Spasojević Dj, Tadić B. Tuneable hysteresis loop and multifractal oscillations of magnetisation in weakly disordered antiferromagnetic–ferromagnetic bilayers. Physica E 2022;142:115319.
[50] Shapoval A, et al. Cyclical trends in critical sandpiles. 2023, inpreparation.
[51] Mitrović Dankulov M, Tadić B, Melnik R. Analysis of worldwide time-series data reveals some universal patterns of evolution of the sars-cov-2 pandemic. Front Phys 2022;10.
[52] Dong E, Ratcliff J, Goyea TD, Katz A, Lau R, Ng TK, et al. The Johns hopkins university center for systems science and engineering Covid-19 dashboard: Data collection process, challenges faced, and lessons learned. Lancet Infect Dis 2022;22(12):e370–6.
[53] Tadić B. MySpace. SAGE Publications, Inc.; 2018.
[54] Thelwall M, Buckley K, Paltoglou G, Cai D, Kappas A. Sentiment strength detection in short informal text. J Am Soc Inf Sci Technol 2010;61(12):2544–58.
[55] V. Gligorijević and M. Šuvakov and B. Tadić.
[56] Andjelković M, Tadić B, Mitrović Dankulov M, Rajković M, Malnik R. Topology of innovation spaces in the knowledge networks emerging through questions-and-answers. PLOS ONE 2016;11(5):1–17.
[57] Szell M, Thurner S. Measuring social dynamics in a massive multiplayer online game. Social Networks 2010;32(4):313–29.
[58] Hu J, Gao J, Wang X. Multifractal analysis of sunspot time series: The effects of the 11-year cycle and fourier truncation. J Stat Mech Theory Exp 2009;2009(02):P02066.
[59] Tadić B, Melnik R. Modeling latent infection transmissions through biosocial stochastic dynamics. PLoS One 2020.
[60] Tadić B, Melnik R. Microscopic dynamics modeling unravels the role of asymptomatic virus carriers in sars-cov-2 epidemics at the interplay between biological and social factors. Comput Biol Med 2021;133:104422.
[61] Muller S, Balmer M, Charlton W, Ewert R, Neumann A, Rakow C, et al. A realistic agent-based simulation model for Covid-19 based on a traffic simulation and mobile phone data. Phys Soc 2020. ArXiv.
[62] Spasojević D, Bukvić S, Milošević S, Stanley G. Barkhausen noise: Elementary signals, power laws, and scaling relations. Phys Rev E 1996;54:2531.
[63] Janićević S, Laurson L, Måløy KJ, Santucci S, Alava M. Interevent correlations from avalanches hiding below the detection threshold. Phys Rev Lett 2016;117:230601.
[64] Spasojević Dj, Mijatović S, Navas-Portella V, Vives E. Crossover from three-dimensional to two-dimensional systems in the nonequilibrium zero-temperature random-field Ising model. Phys Rev E 2018;97:012109.
[65] Tebaldi C, De Menech M, Stella AL. Multifractal scaling in the bak-tang-wiesenfeld sandpile and edge events. Phys Rev Lett 1999;83:3952–5.
[66] Tadić B, Priezzhev V. Scaling of Avalanche queues in directed dissipative sandpiles. Phys Rev E 2000;62:3266–75.
[67] Chang T, Wu C-c. Rank-ordered multifractal spectrum for intermittent fluctuations. Phys Rev E 2008;77:045401.
[68] Tsallis C. The nonadditive entropy sq and its applications in physics and elsewhere: Some remarks. Entropy 2011;13(10):1765–804.
[69] Pavlov AN, Anishchenko VS. Multifractal analysis of complex sisgnals. Phys–Uspekhi 2007;50:819–34.
[70] Kantelhardt JW, et al. Multifractal detrended fluctuation analysis of nonstationary time series. Physica A 2002;316:87–114.
[71] Tadić B. Multifractal analysis of Barkhausen noise reveals the dynamic nature of criticality at hysteresis loop. J Stat Mech Theory Exp 2016;6(6):063305.
[72] Kantelhardt JW, Zschiegner SA, Koscielny-Bunde E, Havlin S, Bunde A, Stanley HE. Multifractal detrended fluctuation analysis of nonstationary time series. Physica A 2002;316(1):87–114.
[73] Pavlov AN, Anishchenko VS. Multifractal analysis of complex signals. Phys-Usp 2007;50(8):819–34.
[74] Tkachenko AV, Maslov S, Wang T, Elbana A, Wong GN, Goldenfeld Nigel. Stochastic social behavior coupled to Covid-19 dynamics leads to waves, plateaus, and an endemic state. ELife 2021;10:e68341.